The isometric knee extension moment-angle relationship: experimental data and predictions based on cadaver data

Meijer, K.; Bosch, P.; Bobbert, M.F.; van Soest, A.J.; Huijing, P.A.J.B.M.

published in
Journal of Applied Biomechanics
1998

DOI (link to publisher)
10.1123/jab.14.1.62

document version
Publisher's PDF, also known as Version of record

JOURNAL OF APPLIED BIOMECHANICS, 1998, **14**, 62-79

The Isometric Knee Extension Moment–Angle Relationship: Experimental Data and Predictions Based on Cadaver Data

Kenneth Meijer, Peter Bosch, Maarten F. Bobbert, Arthur J. van Soest, and Peter A. Huijing

The influence of parameter values (i.e., fiber optimum lengths and moment arms) and simplification of the geometry of a Hill-type muscle model on the prediction of normalized maximal isometric knee extension moment to knee joint angle relationship was studied. For that purpose, the geometry of m. quadriceps femoris was modeled in considerable detail, and all parameter values were determined on one set of cadaver specimens that had been selected for muscular appearance. The predicted relationship was compared to that measured in human subjects over the full range of physiological knee angles, and a good correspondence was found (r = .96). The good correspondence could be attributed to the substitution of realistic parameter values into the model. Incorporating complex muscle geometry into the model resulted in a small additional improvement of the prediction. It was speculated that the variation in results of cadaver measurements among studies reflects true differences caused by individuals' levels of physical activity in the period preceding death.

Key Words: m. quadriceps femoris, muscle model, geometry, human cadavers

Insight into the factors determining performance of motor tasks will benefit practitioners in athletics and rehabilitation. It is generally recognized that performance depends on properties of the musculoskeletal system and on control, with the effects of control being determined by the stimulation patterns that the nervous system sends to the muscles. In order to gain insight into the importance of system properties and control, it is necessary to systematically manipulate these factors and monitor the effects on performance. Unfortunately, system properties cannot be changed in living subjects for obvious reasons, and subjects are unable to systematically manipulate their control. For that reason, researchers have turned to models of the neuromusculoskeletal system.

These models may be constructed such that the input consists of muscle stimulation patterns and the output is the movement and therewith the performance on the task (Levine,

K. Meijer and P.A. Huijing are with the Institute for Biomedical Engineering, University of Twente, Enschede, The Netherlands. P. Bosch, M.F. Bobbert, A.J. van Soest, and P.A. Huijing are with the Department of Functional Anatomy, Faculteit Bewegingswetenschappen, Vrije Universiteit, Amsterdam. Direct correspondence to Maarten F. Bobbert, Vrije Universiteit, Vakgroep Functionele Anatomie, Faculteit der Bewegingswetenschappen, v.d. Boechorststraat 9, 1081 BT Amsterdam, The Netherlands.

Definitions

F_f	muscle fiber force (N); force along the line of pull of muscle fibers
F'_f	normalized muscle fiber force
$F_{f,y}$	muscle force (N); force along the line of pull of the (quadriceps) tendon
$F'_{f,y}$	normalized muscle force
l_{mt}	muscle-tendon complex length (cm); distance between origin and insertion
l_f	muscle fiber length (cm)
$l_{f,y}$	projection of l_f on the line of pull of the (quadriceps) tendon
$l_{f,o}$	muscle fiber optimum length; that length where the isometric force is maximal
l_t	tendon length (cm); length of tendinous tissue in series with muscle fibers
l_t	tendon rest length; tendon length corresponding to zero force
k	stiffness constant of tendon ($N \cdot cm^{-2}$)
α	pennation angle of m. rectus femoris (rad)
α_o	pennation angle of m. rectus femoris at fiber optimum length (rad)
R	radius (cm) of a cylinder representing femur and m. quadriceps femoris
β	angle (rad) in the transverse plane between two lines, one joining the center of the cylinder with the origin of the muscle fiber, the second joining the center of the cylinder with the insertion of the muscle fiber
a_k	moment arm at the knee joint (cm)
a_h	moment arm at the hip joint (cm)
A0…An	polynomial coefficients
θ_k	knee angle (rad)
θ_h	hip angle (rad)
M_k	maximal active isometric moment at the knee joint ($N \cdot m$)
M'_k	normalized for the maximum value

Zajac, Belzer, & Zomlefer, 1983; Pandy, Zajac, Sim, & Levine, 1990; Soest, Schwab, Bobbert, & Ingen Schenau, 1993). Models of the neuromuscular system are used to study explosive movements such as vertical jumping (e.g., Soest et al., 1993).

In modeling enterprises, two factors are important. The first is model complexity: Depending on the goal, models should be as simple as possible. This will limit the computational costs and enhance analysis (insights may be lost if the number of parameters is excessive). This is especially true in modeling muscles, where determining parameter values is a serious problem because no experiments can be performed on isolated human muscles. To find an optimal tradeoff between model complexity and accuracy, several investigators have used Hill-type muscle models (e.g., Pandy et al., 1990; Soest et al., 1993) consisting of a contractile component and a series elastic component. In these models, the muscle fibers often run in a straight line from origin to insertion, and any effects of architectural aspects (Huijing & Woittiez, 1984; Zuurbier & Huijing, 1992) are neglected.

The second important factor is the parameter values used: Values for the required parameters of the muscles themselves, and the way they are embedded into the skeleton, are often extracted from information presented in the literature. However, in the literature, substantial variation occurs in the values of each single parameter, which may be due either to methodological differences or to true anthropometric differences among the cadaver specimens investigated. In the final selection of parameter values used, information has to be combined from different studies and thus from different cadaver specimens. This

may be undesirable because parameters may covary, as suggested by Spoor, Leeuwen, Meulen, and Huson (1991). An additional problem is that cadaver specimens are usually from elderly individuals, who sometimes have been confined to bed for a long time. For example, Cutts and Seedhom (1993) showed that there is a considerable difference in absolute values for the m. quadriceps between healthy subjects and cadaver specimens, although Cutts and Seedhom did not observe differences in ratios.

In the study of vertical jumping, one muscle of the model, the m. quadriceps, plays an important role. This muscle has a very complex geometry with fibers that have their origin at the dorsal side of the femur and their insertion on the patellar tendon at the ventral side of the femur. Further, a wide range of parameter values is encountered, for example, for the mm. vasti, fiber optimum length values from 6.4 to 8.7 cm have been reported (Yamaguchi, Sawa, Moran, Fessler, & Winters, 1990).

The purpose of this study was to decide which of the two factors mentioned above is most important in modeling enterprises. For this purpose, three models of the m. quadriceps were devised. Models 1 and 2 were identical except for the origin of the parameter values. For Model 1 all parameter values were obtained from the literature, and for Model 2 all parameter values were determined from one set of cadaver specimens. In Model 3 we took into account the rather complex architecture of the m. quadriceps; all the parameters were determined on the same set of cadavers as used for Model 2. We evaluated these models by comparing them to experimental knee extension moment angle relationships.

Methods

Subjects and Experimental Protocol

Four physically active male subjects (age 22–24 years, mass 62–71 kg, height 1.80–1.87 m) participated in the dynamometer experiments. Informed consent was obtained from all of them in accordance with the policy statement of the American College of Sports Medicine. The subjects performed isometric contractions on a Kinetic Communicator (KinCom) dynamometer (Chattecx Corp., Chattanooga, TN). The reliability of this device is documented elsewhere (Tredinnick & Duncan, 1988). The experimental protocol was similar to the one used by Herzog, Hasler, and Abrahamse (1991). The warm-up consisted of a series of submaximal dynamic contractions on the dynamometer, two stretch exercises, and three submaximal isometric contractions. Subsequently, the subjects performed maximal isometric contractions at 14 different knee angles between 0.9 rad and π rad in random order (hip joint angle was 1.5 rad). Joint angles were defined as enclosed angles with an angle of π rad defined as full joint extension.

The subjects were asked to gradually build up to a maximal contraction and to maintain this for at least 1 s to ensure that the contraction was truly isometric (i.e., that muscle moment and thus muscle fiber length were more or less constant) (Herzog, Hasler, & Abrahamse, 1991). At each knee angle, the passive moment was measured at rest, and the maximum voluntary moment was determined by averaging the moment over the plateau phase. Between two subsequent contractions, the subject was allowed 3 min rest. Each test session ended with a repetition of the first contraction to check for fatigue effects. The measurement was excluded from the analysis if a 10% deviation from the initial moment was found. Three subjects attended two test sessions, and one subject attended only one test session. Active maximum isometric knee extension moments were obtained by subtracting the passive measured moment from the measured voluntary moment. All moments produced by an individual were normalized with respect to the subject's maximum value, and subsequently the normalized moments at each angle were averaged over the subjects.

Model Description

Hill-Type Muscle Model. Two different Hill-type muscle models were used. The first model was a standard Hill-type muscle model that consisted of a contractile component in series with an elastic component. Both components were in the line of work of the muscle. No parallel elastic component was included, because only small passive moments were measured during the experiments on the Kin-Com (see Results section). The second model was a Hill-type muscle model that incorporated a number of geometrical features (e.g., pennation angle).

With these two models, the isometric moment–knee angle relationship was predicted using three different model configurations:

- Model 1: A simplified geometry model (contractile element [CE] and series elastic component [SEC] in line) for which the parameter values were obtained from the literature (Visser, Hoogkamer, Bobbert, & Huijing, 1990; Wickiewicz, Roy, Powell, & Edgerton, 1983)
- Model 2: A simplified geometry model for which the parameter values were obtained from the present study
- Model 3: A complex geometry model for which the parameters values were obtained from the present study

To derive values for the parameters describing the force–length relationship of the two components, the properties of the contractile component were attributed to the sarcomeres and the properties of the series elastic component were attributed to tendinous tissue in series with the sarcomeres. We assumed that all muscle fibers within the muscle have the same number of sarcomeres in series and "see" a tendon fiber of the same length (the tendon fiber runs through what is macroscopically called aponeurosis). Furthermore, we assumed that all fibers attain their optimum length at the same muscle–tendon complex length; hence, a possible distribution of sarcomere lengths as found by Willems and Huijing (1993) was neglected. Consequently, all fibers were assumed to produce equal forces irrespective of muscle–tendon complex length (cf. Bobbert, Huijing, & Ingen Schenau, 1986). To derive the force–length relationship of the contractile component, the force–length relationship for a human sarcomere was calculated from myofilament lengths as described by Walker and Schrodt (1974). To simplify calculations, the resulting relationship between normalized force and normalized length was subsequently described with a second-order polynomial (Out, Vrijkotte, Soest, & Bobbert, 1996):

$$F' = -0.4 * l_f'^2 + 0.8 * l_f' - 3.0 \quad 0.5 < l_f' < 1.5 \tag{1}$$

where F' is force divided by the maximal isometric force and l_f' is fiber length divided by optimum length, that is, the length where the maximal isometric force occurred (Soest et al., 1993). To get from this normalized relationship to that between muscle fiber force F_f and muscle fiber length l_f, normalized force was multiplied by the normalized PCSA of the individual muscles (PCSA of the muscle divided by PCSA of the entire quadriceps muscle group), and the normalized length was multiplied by muscle fiber optimal length ($l_{f,o}$) determined from the number of sarcomeres in series in the muscle fibers.

Geometrical Model. Many muscle fibers of m. quadriceps femoris originate from the dorsal aspect of the femur; they follow a more or less helical course around the femur and insert into the quadriceps tendon on the ventral side (Alexander & Vernon, 1975). The helical course of the fibers corresponds to a sigmoid projection in the sagittal plane. The

muscle fibers curving around the lateral side belong to m. vastus lateralis, and the ones curving around the medial side belong to m. vastus medialis. Together with muscle fibers of m. vastus intermedius, which arise from the ventral side of the femur, they form a more or less cylinder-shaped muscle cuff. M. rectus femoris, although inserting on the same tendon, runs more or less independently from the mm. vasti from its origin on the pelvic bone. In agreement with this anatomical arrangement, mm. vasti were modeled as one large bipennate unit wrapped around a cylinder-shaped femur, and m. rectus femoris was modeled as a second bipennate unit.

In modeling the unit representing the mm. vasti, we assumed that the muscle fibers run along the shortest path, from their origin on the dorsal side of the femur to their insertion on the quadriceps tendon, around the cylinder-shaped femur (Figure 1, a and b); this assumption corresponds to their helix-shaped course. Note that change in knee angle is not directly related to a change in l_f but rather to a change in $l_{f,y}$, the projection of muscle fiber length on the line of pull of the quadriceps tendon, which runs parallel to the length axis of the cylinder (Figure 1a). When the hollow muscle cylinder is unfolded onto a two-dimensional plane, a triangle is formed by $l_{f,y}$, l_f, and the height of the triangle, with the latter being the product of the radius of the cylinder f,y R and the angle β, in the transverse plane, between the center of the cylinder and the origin and insertion of the muscle fiber (Figure 1b). This triangle represents one half of the vastus muscle cuff. It seems reasonable to assume that β remains constant along the femur and to neglect the elongation of the series elastic tissue between the muscle fiber and its origin on the femur and insertion on the quadriceps tendon. Under these conditions, $l_{f,y}$ can be expressed as a function of l_f:

$$l_{f,y} = \sqrt{l_f{}^2 - (\beta - R)^2} \tag{2}$$

In modeling the unit representing the bipennate m. rectus femoris, we assumed that the distances between each of the two proximal aponeuroses and the insertion on the quadriceps tendon were constant and identical to each other and amounted to the product of muscle fiber optimum length $l_{f,o}$ and the sine of the angle of pennation at muscle optimum length (α_o). If we again neglect the elongation of the series elastic tissue between the muscle fiber and its origin on the proximal aponeurosis and insertion on the quadriceps tendon, and assume that muscle volume remains constant, then $l_{f,y}$ can be expressed as a function of l_f in m. rectus femoris:

$$l_{f,y} = \sqrt{l_f{}^2 - (l_{f,o} * \sin\alpha_0)^2} \tag{3}$$

The calculation of force as a function of length started from the force–length relationship of the muscle fibers (see above). Muscle force can be calculated from fiber force, since muscle work needs to equal fiber work (Otten, 1985, 1988). Thus,

$$F_{f,y} * \delta l_{f,y} = F_f * \delta l_f \tag{4}$$

so that

$$F_{f,y} = F_f * \frac{\delta l_f}{\delta l_{f,y}} \tag{5}$$

In the infinitesimal case, the derivatives of $l_{f,y}$ with respect to l_f may be used. This yields for mm. vasti

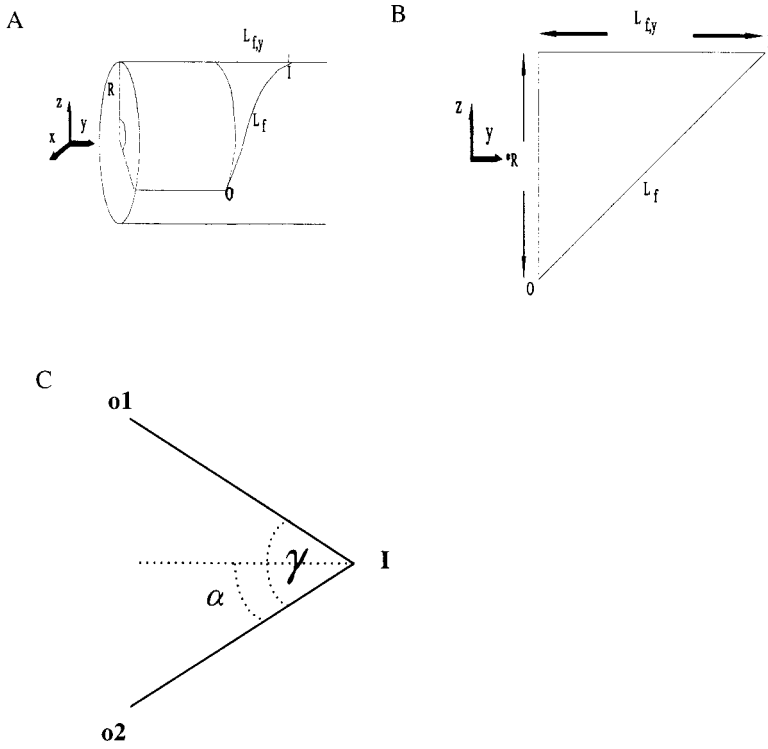

Figure 1 — Schematic representation of mm. vasti geometry. (a) The femur including the mm. vastii muscle cuff was modeled as a cylinder of radius *R*, with muscle fibers of m. vastus medialis and m. vastus lateralis running along the shortest path from their origin at the dorsomedial or dorsolateral aspect of the femur (O) to their insertion on the tendon of m. quadriceps (I). Only a single fiber of one of the m. vastii is drawn. A decrease in the length of the muscle fibers l_f yields a displacement of the tendon of m. quadriceps, which is equal to the decrease in the projection of muscle fiber length on the longitudinal axis (*y*-axis) of the cylinder ($l_{f,y}$). ß is the angle between a line joining the center of the cylinder with the origin of the muscle fiber, and a line joining the center of the cylinder with the insertion of the muscle fiber. (b) When the muscle cuff is unfolded to a plane, a triangle is formed that allows for calculation of $l_{f,y}$ from l_f. (c) Schematic representation of the rectus femoris geometry. Two fiber bundles converge to one insertion (o1-I and o2-I). To determine the angle of pennation, the angle γ is determined from the coordinates of the points o1, o2, and I. This angle is then divided by 2 to get the value for α.

$$F_{f,y} = F_f * \sqrt{\frac{l_f^{\,2} - (\beta * R)^2}{l_f^{\,2}}} \tag{6}$$

and for m. rectus femoris

$$F_{f,y} = F_f * \sqrt{\frac{l_f^{\,2} - (l_{f,o} * \sin\alpha_o)^2}{l_f^{\,2}}} \tag{7}$$

Tendon force was assumed to depend quadratically on tendon elongation, so that tendon length could be determined from muscle force:

$$l_t = \sqrt{\frac{F_{f,y}}{k}} + l_{t,o} \tag{8}$$

with stiffness constant k being chosen such that tendon elongation was 4% of tendon rest length ($l_{t,o}$) when a maximal isometric contraction was performed at optimum muscle length (Bobbert, Ettema, & Huijing, 1990). Length of the whole muscle tendon complex l_{mt} was defined as the sum of l_t and $l_{f,y}$.

The last step is the transformation of muscle length and force to knee angle and moment. For that purpose, the relationship between l_{mt} and θ_k needs to be known for mm. vasti and m. rectus femoris. The first derivative of this relationship with respect to θ_k yields the moment arm of the quadriceps tendon at the knee (Bobbert et al., 1986), which is needed to calculate the knee extension moment from quadriceps force.

Order of Computations. Obtaining individual points for the predicted relationship between M_k and knee joint angle involved the following steps:

1. Selection of a value for l_f and calculation of $l_{f,y}$ according to Equations 2 (mm. vasti) and 3 (m. rectus femoris)
2. Calculation of F_f according to Equation 1
3. Calculation of $F_{f,y}$ according to Equations 6 (mm. vasti) and 7 (m. rectus femoris)
4. Calculation of l_t according to Equation 8
5. Summation of $l_{f,y}$ and l_t to obtain l_{mt}
6. Calculation of θ_k corresponding to l_{mt} from Step 5
7. Calculation of M_k corresponding to $F_{f,y}$ from Step 3

The calculations for mm. vasti require values for the parameters R, l_f, β, $l_{f,o}$, $l_{t,o}$, and PCSA, and the relationship between l_{mt} and θ_k needs to be determined. For m. rectus femoris, values have to be obtained for α_o, l_f, $l_{f,o}$, $l_{t,o}$, and PCSA, and l_{mt} needs to be determined as a function of θ_k, θ_h.

Determination of Parameter Values

Cadaver Specimens and Dissection Procedures. Four lower extremities of two embalmed human cadaver specimens, which had been selected because of a good muscular appearance by an expert anatomist, were used to determine parameter values. The cadaver specimens were embalmed for dissection purposes shortly after death, by infusion of a solution containing 10% formaldehyde, 5% chloral hydrate, 3% sal carolineum, 0.2% salicyclic acid, and 0.1% thymol into the femoral artery. They were kept covered by a 50% ethanol solution, containing 0.025% thymol, for a minimum of 8 months. The cadaver specimens were cleared from subcutaneous fat, fascia, blood vessels, and nerves, and all the muscles except m. quadriceps femoris were removed from the thigh to make the origins and insertion of this muscle visible. The dissection procedure did not change the shape of the quadriceps. The specimen was placed in a stiff metal framework similar to the one used by Visser et al. (1990), and the pelvis and femur were fixed. The knee angle was defined as the angle between two lines, one from the most lateral aspect of the trochanter major to the lateral femoral epicondyle and the other from the lateral tibial epicondyle to the lateral malleolus. Screws were inserted into the bone at these anatomical landmarks for accurate determination of the knee angle (see below).

Coordinate Frame. From the assumptions that mm. vasti form a symmetrical bipennate muscle and that the femur and mm. vasti have the shape of a cylinder, it follows that the line of pull of m. quadriceps femoris is parallel to the longitudinal axis of the cylinder. To determine the orientation of this longitudinal axis, a palpator was mounted on the stiff metal frame containing the leg. This device allowed us to measure three-dimensional (3-D) coordinates of points (Pronk & Helm, 1991). In a plane perpendicular to the estimated longitudinal axis of the femur with muscles, a stiff cord with equally spaced points was placed around the proximal part of the femur. The 3-D coordinates of approximately 30 points on the cord were determined. A least-squares procedure was used to fit a circle through these coordinates, and the center of the circle and its radius were determined. This procedure was then repeated with the cord around the middle and distal parts of the femur with muscles. Due to the limited operating range of the palpator, we measured each circle from both the medial and the lateral side of the leg. Thus we measured a total of six circles. Using the vector from the center of the proximal circle to the center of the distal circle, and the vector from the center of the proximal circle to a point on the circle, we defined an orthogonal coordinate system (Berme & Cappozzo, 1990) with its origin in the center of the distal circle and its *y*-axis corresponding to the longitudinal axis of the femur with muscles. All data points subsequently collected were transformed to this local coordinate system.

Determination of R, β, and α_o. The radius of the cylinder formed by the femur and the m. quadriceps (R) was defined as the average radius of the six circles fitted to the data. The angle β (Figure 1, a and b) can be determined as

$$\beta = \sqrt{\frac{l_f^{\,2} - l_{f,y}^{\,2}}{R}} \tag{9}$$

Because fiber lengths cannot be determined *in situ*, the length of fiber bundles was used instead. Fiber bundles were selected at standardized locations from m. vastus lateralis (at 15, 30, and 50% of muscle belly length, measured from the distal end of the muscle belly) and m. vastus medialis (at 5, 20, and 45% of muscle belly length, measured from the distal end of the muscle belly). Thus, for each leg we measured six fiber bundles. The coordinates of the origin and insertion of each bundle and those of 20 equally spaced points on the bundle were collected. The total length of each bundle, which was substituted for l_f, was calculated by adding the lengths of the vectors pointing from one point to the next point on the bundle. Subsequently, $l_{f,y}$ was obtained by subtracting the *y*-coordinates of the origin and the insertion of the bundle. This procedure was carried out for each fiber bundle, and values for β were determined from the values obtained for fiber bundle lengths at each of the three locations for vastus medialis and lateralis and were averaged for use in the model.

To determine α_o for the bipennate m. rectus femoris (the angle of pennation at optimum length), we determined the coordinates of origin and insertion of two converging bundles at 60% of muscle belly length (measured from the distal end of the muscle belly) with the aid of the palpator (Figure 1c: Bundles o1-I and o2-I). The angle between the two vectors representing the longitudinal axes of these bundles (γ) was then calculated and divided by 2 to obtain α. Assuming that the distance between the medial and lateral tendon plates remained constant, we obtained α_o as follows:

$$l_{f,o} * \sin\alpha_o = l_f * \sin\alpha \tag{10}$$

The length of the bundle (l_f) was estimated from the length of the vector pointing from the origin to the insertion of the bundle. After the measurements, the selected bundles were removed at standardized locations from m. vastus lateralis, m. vastus medialis, and m.

rectus femoris and were stored for determination of the number of sarcomeres in series and therewith $l_{f,o}$.

Determination of Relationships Between l_{mt} and Joint Angles θ_h and θ_k. We determined the relationship between l_{mt} and joint angles by cutting the muscles and measuring the gap width between the corresponding ends of fiber bundles over a range of joint angles, a method first described by Grieve, Pheasant, and Cavanagh (1978). First, two markers were longitudinally placed 1 cm apart on the middle of fiber bundles of six parts of m. quadriceps femoris: m. vastus intermedius, lateral and medial part of the vastus medialis, lateral and medial part of the vastus lateralis, and m. rectus femoris. Subsequently, a transverse cut was made through each of these parts, so that the two ends had one marker each. The distal ends of m. quadriceps still contained some intact deep fibers that originated from the femur, which were cut to allow for flexion of the knee joint. The hip angle was now set at π rad and the knee angle was varied from π rad to 1.5 rad in steps of approximately 0.1 rad. At each configuration, the coordinates of the landmarks defining the knee angle were determined with the palpator, the fiber bundles containing corresponding markers were aligned, and the gap width in each muscle belly was measured, again using the palpator. After this set of measurements, an additional set was performed for m. rectus femoris only, with the knee angle fixed at 1.5 rad and hip angles ranging from π rad to 1.5 rad.

All gap lengths were expressed in percentages of upper leg lengths (i.e., distance between greater trochanter major and epicondylis lateralis). Polynomials were fitted to all individual relationships between gap lengths and joint angle(s) using least squares. The fitting started with a first-order polynomial. We then increased the order of the polynomial to see if this yielded a statistically significant increase ($p < .05$) of the explained variance. The constant A0 of the polynomial was replaced by a reference length estimated from the muscle tendon complex length at knee and hip angles of π rad. We then calculated moment arms as a function of joint angles by taking the first derivative of the polynomials with respect to joint angle (Bobbert et al., 1986). After completing these experiments, we removed the muscles to determine muscle volumes (see below).

Determination of $l_{f,o}$. Optimal length of muscle fibers, $l_{f,o}$, for m. vastus lateralis, m. vastus medialis, and m. rectus femoris was determined using the method of Huijing (1985). First, the stored fiber bundles were separated into a number of smaller bundles. These smaller bundles were rinsed in water for 1 hr to remove as much of the embalming fluid as possible. Subsequently, they were immersed in a 26% HNO_3 solution for 4 hr to remove connective tissue. Next the bundles were stored in a 50% glycerine solution. Under a binocular (magnification 6×), three single fibers were teased out from each bundle, which were placed on a microslide. To ensure that complete fibers were taken out of the bundle, each preparation was checked for characteristic invaginations at both ends. Fiber length was determined by measuring the length of the projected fiber (magnitude 20 times) with a calibrated curvimeter, and in each fiber the number of sarcomeres in series was counted in samples of 80 μm taken every 2,400 μm along the fiber. From these data, the total number of sarcomeres in each muscle fiber was estimated. To obtain $l_{f,o}$, this number was multiplied by a sarcomere optimum length of 2.73 mm (Herzog, Abrahamse, & Keurs, 1990; Walker & Schrodt, 1974).

Determination of PCSA. Volumes of mm. vasti and m. rectus femoris were determined by submersion in a water tank and measuring water displacement with a gauge glass. To obtain values for PCSA, muscle volume was divided by $l_{f,o}$.

Determination of $l_{t,o}$. A value of tendon rest length $l_{t,o}$ is difficult to determine by measurements in cadaver specimens. Therefore, values for $l_{t,o}$ for mm. vasti and m. rectus femoris were obtained with an optimization procedure, in which the least squares difference

between the measured and predicted relationships between M_k and knee angle was minimized (Simplex algorithm; Nelder & Mead, 1964).

Results

Dynamometer Experiments

In Figure 2, the group means and standard deviations for normalized knee extension moments have been plotted as a function of knee angle. The curves were taken to represent the effect of knee angle (and therewith muscle length) on the isometric moments at maximal voluntary contraction of the muscles. The moments measured in the control contractions were within 10% of their initial value. Thus, it was concluded that muscular fatigue had not biased the experimental results. The isometric moment–angle relationship of the individuals deviated maximally 15% from the mean curve. The maximum moment of the subjects amounted to 223 N · m on average. Passive moments are not shown; even at a knee flexion of 0.7 rad, they were less than 10% of the active moment at that angle. Similar results for passive moments were obtained by Pierrynowsky and Morrisson (1985). We decided, therefore, to neglect the passive moments altogether.

Values for Model Parameters

In m. rectus femoris, the number of sarcomeres in series in muscle fibers amounted to 28,358 (±1,997), and α was 0.28 (±0.03) rad. The volume of the muscle belly was 154 (±29) cm^3, and PCSA was calculated to be 20 (±3) cm^2. In m. vastus medialis, the average number of sarcomeres in series was 41,796 (±5,338) and in m. vastus lateralis it was 40,716 (±4,806), with the difference of only 3% not statistically significant ($p > .05$). No statistically significant differences were found between fibers selected from different positions within each muscle belly. Angle β was 1.69 (±0.22) rad in m. vastus lateralis and

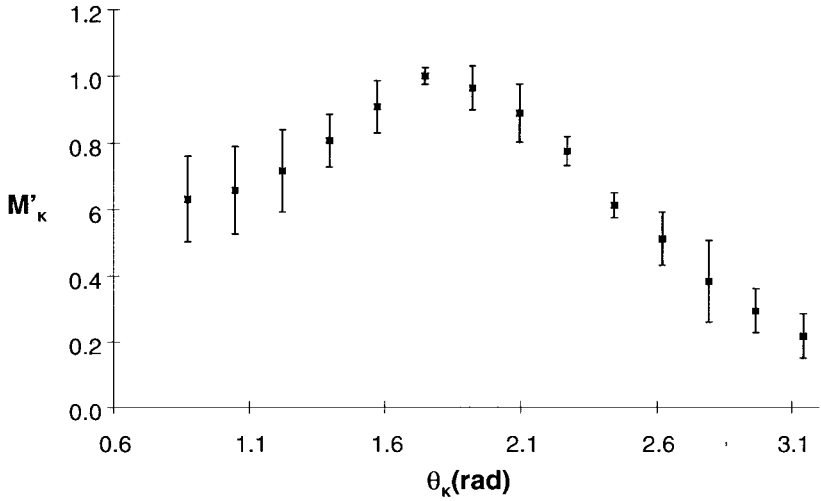

Figure 2 — Mean values of normalized active isometric knee extension moment (M'_k) as a function of knee joint angle (θ_k), produced by four subjects during maximum-effort contractions on a dynamometer (■). Vertical bars indicate standard deviation.

1.42 (±0.4) rad in m. vastus medialis. The total volume of m. vastus lateralis, m. vastus medialis, and m. vastus intermedius combined amounted to 1,134 (±141) cm^3, and the total PCSA was calculated to be 101 (±9) cm^2.

Table 1 shows the polynomial coefficients for the relationship between gap lengths and joint angles as well as the correlation coefficients between polynomially fitted data and measured data. Lengths were expressed in percentages of upper leg length, which was defined as the distance between trochanter major and epicondylis lateralis and amounted to 0.4 m on average (±0.01). For the m. vastus intermedius, a second-order polynomial produced a significantly better fit than a first-order one, although the magnitude of the higher order effects was relatively small. Moment arms were deduced from the changes in gap length and joint angles. For the m. vastus intermedius, we determined the average moment arm over the studied knee joint angle range. The mean value for moment arms was used for two reasons: The second-order effect was very small, and the relationships had to be extrapolated beyond the knee angle range used in the cadaver measurements. The choice to use mean moment arm seems to be justified by the work of Out et al. (1996), who found that simulation results of moment–angle relationships are very sensitive for mean moment arm and much less sensitive for any higher order effects. It would be interesting to correlate numbers of sarcomeres in series and moment arms at the knee joint. However, since the variation in upper segment lengths of the specimens used was very small (0.4 ± 0.01 m), it will be hard to find a relationship.

Surprisingly, the moment arms of m. rectus femoris and m. vastus intermedius were somewhat larger than those of m. vastus lateralis and m. vastus medialis. This was also noticed by Visser et al. (1990) and is probably caused by the geometry of the system as described in this study, that is, the fact that the muscle fiber bundles of m. vastus medialis and m. vastus lateralis, which were selected to measure the gap length, do not run parallel to the line of pull of the quadriceps tendon. In other words, for these fiber bundles it

Table 1 Values for Polynomial Coefficients Describing the Relationships Between Muscle–Tendon Complex Length (l_{mt}) and Joint Angles (θ), and the Correlation Coefficients (*r*) Between Fitted Data and Measured Data

	Polynomial coefficients				
	A_0	A_1	A_2	*r*	*a* (cm)
VLL	0.326414	–0.09753	—	0.97	3.9
VLM	0.352259	–0.107345	—	0.98	4.3
VI	0.2552503	0.011535	–0.021534	0.97	4.5
VML	0.325122	–0.096544	—	0.97	4.3
VMM	0.351578	–0.106865	—	0.98	3.9
RFk	0.360705	–0.113512	—	0.99	4.5
RFh	–0.033	–0.08177	—	0.95	3.3

Note. Polynomials are of the form $I_{mt} = A_0 + A_1 \cdot \theta + A_2 \cdot \theta^2$. Angles are expressed in degrees and I_{mt} is expressed in percentage of upper leg length (defined as the distance between trochanter major and epicondylis lateralis), which amounted to 0.400 m on average. Absolute moment arms, averaged over the range of knee angles investigated, are shown as well.

could be possible that we directly measured the effect of changes in knee angle on l_f instead of on $l_{f,y}$. This is because the two parts of the muscle fiber bundle were aligned before we measured gap length, which could result in a systematic underestimation of the moment arm as is indicated by the lower moment arms for m. vastus lateralis and m. vastus medialis.

Model Predictions

The fiber optimum lengths of m. vastus lateralis and m. vastus medialis were almost equal, an observation similar to that made by Herzog et al. (1990). Since fiber optimum length is an important factor determining the isometric moment–angle relationship, the decision to model mm. vasti as one large bipennate muscle and to lump the results of the individual parts in the model seems justified. Table 2 shows the lumped parameter values substituted in the model for mm. vasti as well as the parameter values for m. rectus femoris for the three model configurations. In the model, the moment arm of the quadriceps tendon (i.e., that of m. vastus intermedius) was substituted for the moment arm of mm. vasti. For the vastus intermedius, the gap lengths were measured in the line of pull of the muscle; hence, its moment arm is assumed to be the most reliable estimate. Figure 3 shows the simulated isometric moment–angle relationships for the three different model configurations, together with the experimental results. Model 1, with parameter values obtained from the literature, was not capable of generating an extension moment over the range of physiological knee angles (Figure 3). Incorporating into Model 2 parameter values for moment arm and optimum lengths that were obtained from our cadaver study improved the simulation results considerably, as illustrated by Figure 3. Incorporating a more realistic muscle geometry in Model 3 considerably broadened the moment–angle relationships of m. vastii and m. rectus femoris. Surprisingly, this resulted in only a small additional improvement of the model predictions. Comparison of Figure 3 shows that for both Models 2 and 3, there is a good agreement between the predicted curves and the experimentally obtained

Table 2 Values Substituted in the Model for M. Rectus Femoris (RF) and Mm. Vasti (VA)

		Model parameters							
Model		$l_{f,o}$ (cm)	a_k (cm)	a_h (cm)	PCSA	$l_{t,0}$ (cm)	R (cm)	β (rad)	α_o (rad)
1	VA	8.87	5.4	—	0.85	26.7	—	—	—
	RF	7.3	5.6	3.5	0.15	33.3	—	—	—
2	VA	11.3	4.4	—	0.83	25.8	—	—	—
	RF	7.8	4.5	3.3	0.17	36.8	—	—	—
3	VA	11.3	4.4	—	0.83	28.1	4.04	1.5	—
	RF	7.8	4.5	3.3	0.17	35.5	—	—	0.35

Note. Physiological cross-sectional areas (PCSA) were normalized by the combination of RF and VA. Values for tendon rest length ($l_{t,o}$) are different for the model with complex geometry and the model with simplified geometry. See list of abbreviations for meaning of parameters.

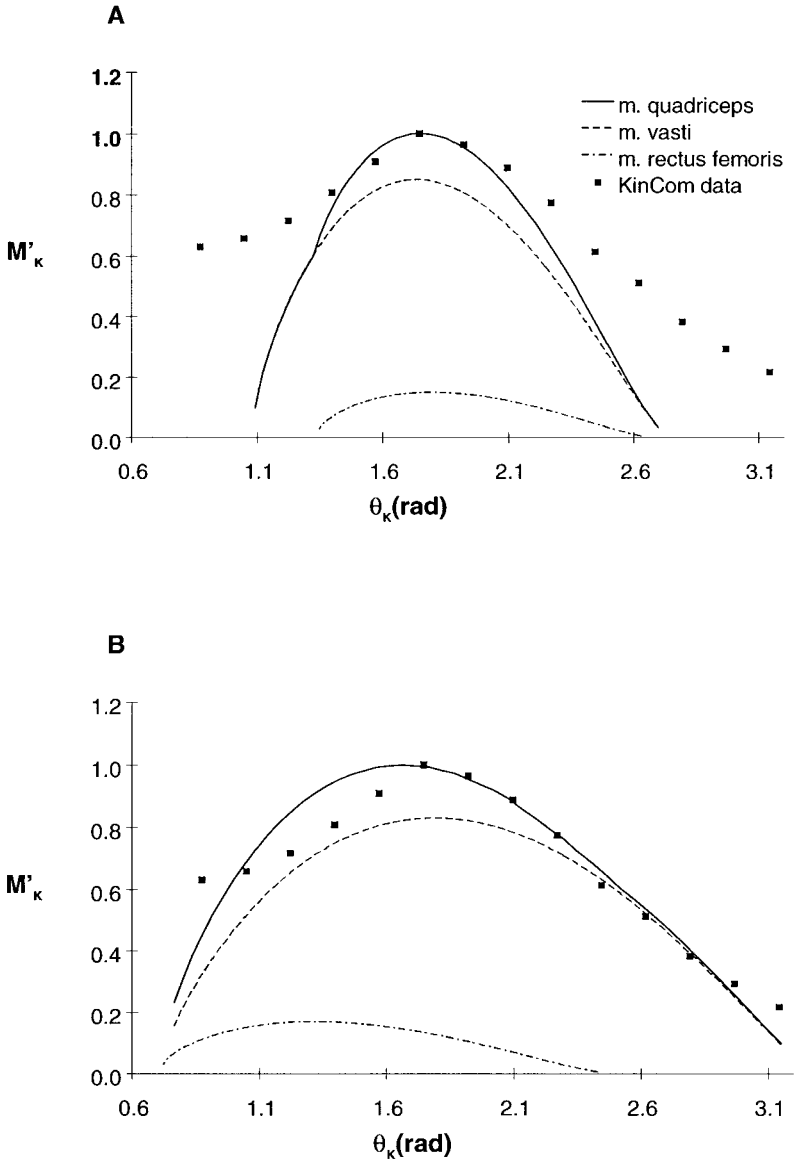

Figure 3 — Predicted normalized active isometric knee extension moment (M'_k) as a function of knee joint angle (θ_k) for three different models of m. quadriceps femoris, together with the mean experimental data. The individual contributions of m. rectus femoris and m. vastii to M'_k are also shown (— = m. quadriceps; - - - = m. vastii; - · - = m. rectus femoris; ■ = mean Kin-Com data also presented in Figure 2). (a) Model 1, a simplified geometry model with parameter values obtained from the literature (Visser et al., 1990; Wickiewicz et al., 1983). (b) Model 2, a simplified geometry model with parameter values determined in the present study. ***(continued)***

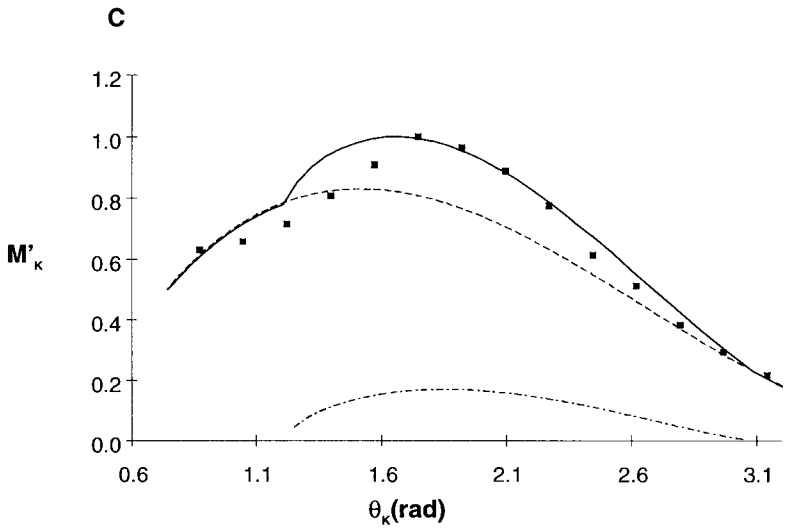

Figure 3 — (c) Model 3, a complex muscle geometry model for which the parameter values were determined in the present study.

curve (r = .96 for simplified geometry model and r = .98 for complex geometry model). The predicted curve deviated maximally 15% from the experimental curve. Note that the knee angle at which the m. vastii and the rectus femoris attain their peak moment depends on the model assumption. In Model 2 they amount to 1.8 rad for m. vastii and 1.3 rad for m. rectus femoris, while in Model 3 they amount to 1.5 rad and 1.85 rad, respectively (Figure 3). This is caused by the optimization method, which varies tendon slack length of both muscles to find the best model description of the experimental data.

Discussion

In models of the human neuromusculoskeletal system, muscles are represented in a way that seems to do little justice to the geometry of the real system. In the present study we evaluated the influence of model simplifications and parameter values on model performance. For this purpose we compared three model configurations on their ability to predict the experimental isometric knee extension moment–angle relationship.

The model with the simplified geometry and parameter values obtained from the literature (Model 1) failed to predict knee extension moments over the range of physiological knee flexion angles (Figure 3). In contrast, the other two model configurations gave good predictions. The complex geometry model (Model 3) gave the best prediction of the experimental data (Figure 3). However, the simplified geometry model for which the input parameters were determined in the present study (Model 2) performed almost equally well (Figure 3). Thus, it could be concluded that for predicting the isometric knee extension moment–angle relationship, incorporating a complex geometry into the muscle model is not very important. However, this conclusion should be made with some reservations, because the knee angle where the models of m. vastii and m. rectus femoris produce their maximal moment depends on the model assumptions. In Model 2, the m. rectus femoris reaches its peak moment in a more flexed position of the knee compared to Model 3

(1.3 and 1.8 rad, respectively). This difference results from the optimization method used to determine the tendon rest lengths. In Model 2, the optimization method chose the tendon rest length of the m. rectus femoris such that this muscle compensates for the reduced m. vastii moment at extensive knee flexion. In Model 3, the m. vastii is capable of generating a sufficient moment over the studied range of knee angles. Here the m. rectus femoris generates a moment over the midrange of knee angles. Thus, before discarding muscle geometry as an important model parameter, we should answer the question, How do these two synergistic muscles contribute to the "in vivo" knee extension moment?

Unfortunately, information regarding this question is scarce. Herzog et al. (1990) estimated the position of the biarticular m. rectus femoris by measuring the knee extension moment angle relationship for two different hip angles (sitting and lying position). At a hip angle of 1.5 rad (sitting position), they predicted that m. rectus femoris produced its peak moment at approximately 1 rad. This agrees quite well with the prediction of our Model 2. However, they optimized the parameter values of their model. Hence, their results may also depend on their model assumption. It is noteworthy that they also used a model with simplified muscle geometry, which may explain the agreement of their result with that of our Model 2. An additional problem is that there may be significant intersubject differences in the contribution of synergistic muscles to the joint moment. For example, Herzog, Guimares, et al. (1991) found evidence for significant differences in the angle at which rectus femoris produces its peak moment between different types of athletes. This may point to muscular adaptations to functional demands.

For our case, the problem of the relative contribution of synergistic muscles to joint moments may be solved by looking at the passive moments. In the experimental data, the passive moments were very small even at extreme knee flexion angles (0.7 rad). This observation fits better with the results of Model 2 than with those of Model 3. In Model 3, m. rectus femoris reached active insufficiency at a knee angle of approximately 1.10 rad. In general, passive force in the muscle starts to develop beyond the optimal length. Passive force increases exponentially with muscle length, and at the length where the muscle reaches active insufficiency it will be larger than the maximal active force of the muscle (e.g., Out et al., 1996). Although we did not incorporate passive forces into our muscle model, it is clear from the above rationale that the passive moments in Model 3 would become very large for knee flexion angles smaller than 1.10 rad. In Model 2, however, the passive moments would be relatively small, which corresponds well with the experimental observations. Hence, the position of m. rectus femoris in Model 2 seems to be more likely than that in Model 3. Unfortunately, the angle at which the monoarticular m. vastii produce their peak moment is far more difficult to estimate. Passive force of the m. vastii is estimated to be low in both muscle models; thus, the passive moments cannot be used as discriminators.

It seems that incorporating a complex muscle geometry does not improve the overall model prediction considerably. However, a definite conclusion regarding the importance of muscle geometry can only be drawn when there is insight into the relative contribution of individual muscles to total joint moment.

An important result of the present study is that the performance of the simplified geometry model could be improved considerably if the parameter values measured in the present study were substituted in the model with simplified geometry (cf. Figure 3). A number of factors may be responsible for this improvement. First, it may be possible that muscle parameters and skeletal parameters covary. Physically active persons are generally capable of producing moments over similar ranges of physiological knee angles, although differences in anthropometry might exist. For example, all subjects in our dynamometer experiments exhibited qualitatively similar isometric knee extension angle–

moment relationships. The range of knee angles for which an active moment can be generated is mainly determined by the quotient of fiber optimum length and moment arm. Therefore, it seems plausible that fiber optimum length and moment arm covary, as was suggested by Spoor et al. (1991). The exact relationship between the number of sarcomeres and moment arm, however, is yet to be quantified (Murray, Wyles, Buchanan, & Delp, 1996). In the literature there are reports of considerable differences in parameter values obtained from different cadaver specimens (i.e., An, Hui, Morrey, Linscheid, & Chao, 1981; Yamaguchi et al., 1990). The importance of subject-specific parameters for model performance has been addressed previously (Audu & Davy, 1985). This indicates that it is quite hazardous to collect parameter values from different sources, as is illustrated by the poor performance of our Model 1. However, it is considered safe to collect both muscle and skeletal parameters from the same subject as was done in the present study.

Second, it is possible that the number of sarcomeres decreases when people are confined to bed and no longer use their muscles through the complete range of motion. This speculation is supported by the results of animal studies, in which it has been found that the number of sarcomeres in series decreases during a period of immobilization (Heslinga, Kronnie, & Huijing, 1992). In our study we tried to avoid the possible influence of a subject's physical condition on parameter values. Therefore, we selected the cadaver material for good muscular appearance, which might reflect a physically active life up to the time of death.

Third, the parameter values obtained should not be influenced by any method used. We strongly believe that the product of numbers of sarcomeres in series and sarcomere optimum length is the most reliable estimate for muscle fiber optimum length, because the number of sarcomeres in series is not affected by any method of treatment of the specimens. We also consider our measurement of moment arm reliable since it was not influenced by any assumptions concerning the rotation center of the knee joint.

Because of the care taken to obtain good estimates for parameter values, we believe that the improved prediction of Model 2 compared to Model 1 is mainly due to a better set of parameter values. For example, our muscle fiber length of m. vastii (11.3 cm) was considerably larger than in other studies (8.8 cm reported by Wickiewicz et al., 1983, and 6.3–8.9 cm reported by Yamaguchi et al., 1990); our muscle fiber optimum length for m. rectus femoris was in the upper limits of the range reported by Yamaguchi et al. (1990) (5.5–8.2 cm); and our moment arm (4.5 cm) was smaller than that reported by Visser et al. (1990) (5.4 cm used in Model 1). When these values are used to calculate the range between angle at peak moment and the angle at which active insufficiency is reached, a gain of 0.9 rad is achieved. This will result in the better model prediction. Whether the improvement was caused by determination of all parameter values from the same cadaver population, the selection of the specimens for their muscular appearance, or both could not be distinguished. Herzog, Hasler, and Abrahamse (1991) also found a good agreement between predicted and experimental isometric knee extension moment–angle relationships. Noteworthy is that their values of fiber optimum lengths of m. vastii and m. rectus femoris were similar to the ones determined in the present study.

Concluding Remarks

In the present study, the relationship of maximum normalized isometric knee extension moment to knee joint angle measured in human subjects was predicted quite well with a relatively simple muscle model. The values for all input parameters were determined by measurements on human cadaver specimens that had been selected for a muscular appear-

ance. It was shown that incorporation of a complex geometry does not improve overall model performance. However, it does affect the relative contribution of synergistic muscles to the overall joint moment. Considering the scarce information regarding the contribution of individual muscles to overall joint moment, further research in this area seems warranted. It was also shown that the predictions based on parameter values from one cadaver population yielded better results than the prediction with parameter values obtained from the literature. These better predictions could be the result of obtaining the parameter values from one set of cadaver specimens. In this way we avoided the problems that can occur because of the possibility of covarying parameters. Furthermore, it was speculated that the discrepancies in results of cadaver measurements among studies not so much are caused by differences in methods but reflect true differences caused by the level of physical activity of individuals in the period preceding death. Unfortunately, the status of the musculature of cadavers is usually not described in the literature. There seems to be a need for studies of the effects of physical activity and covariance on the values of parameters that are important determinants of mechanical output of muscle models.

References

Alexander, R.M., & Vernon, A. (1975). The dimensions of knee and ankle muscle and the forces they exert. *Journal of Human Movement Studies*, **1**, 115-123.

An, K.N., Hui, F.C., Morrey, B.F., Linscheid, R.L., & Chao, E.Y. (1981). Muscles across the elbow joint: A biomechanical analysis. *Journal of Biomechanics*, **14**, 659-669.

Audu, M.L., & Davy, D.T. (1985). The influence of muscle model complexity in musculoskeletal motion modelling. *Journal of Biomechanical Engineering*, **107**, 147-157.

Berme, N., & Cappozzo, A. (1990). *Biomechanics of human movement: Applications in rehabilitation, sports and ergonomics*. Worthington, OH: Bertec Corporation.

Bobbert, M.F., Huijing, P.A., & Ingen Schenau, G.J. van (1986). A model of the human triceps surae muscle-tendon complex applied to jumping. *Journal of Biomechanics*, **19**, 887-898.

Bobbert, M.F., Ettema, G., & Huijing, P.A. (1990). Force-length relationship of a muscle tendon complex: Experimental results and model calculations. *European Journal of Physiology*, **297**, 1-7.

Cutts, A., & Seedhom, B.B. (1993). Validity of cadaveric data for muscle physiological cross-sectional area ratios: A comparative study of cadaveric and in-vivo data in human thigh muscles. *Clinical Biomechanics*, **8**, 156-162.

Grieve, D.W., Pheasant, S., & Cavanagh, P.R. (1978). Prediction of gastrocnemius length from knee and angle joint posture. In E. Asmussen & K. Jörgensen (Eds.), *Biomechanics VIA* (pp. 405-412). Baltimore: University Park Press.

Herzog, W., Abrahamse, S.K., & Keurs, H.E.D.J. ter (1990). Theoretical determination of force-length relations of intact human skeletal muscles using the cross bridge model. *Pflügers Archiv*, **416**, 113-119.

Herzog, W., Hasler, E., & Abrahamse, S.K. (1991). A comparison of knee extensor strength curves obtained theoretically and experimentally. *Medicine and Science in Sports and Exercise*, **23**(1), 108-114.

Herzog, W., Guimares, A.C., Anton, M.G., & Carter-Erdman, K.A. (1991). Moment-length relations of rectus femoris muscles of speed skaters/cyclists and runners. *Medicine and Science in Sports and Exercise*, **23**(11), 1289-1296.

Heslinga, J.W., Kronnie, G. te, & Huijing, P.A. (1992). Growth and immobilization effects on sarcomeres: A comparison between gastrocnemius and soleus muscles of adult rats. *Journal of Applied Physiology and Occupational Physiology*, **70**, 49-57.

Huijing, P.A., & Woittiez, R.D. (1984). The effect of architecture on skeletal muscle performance: A simple planimetric model. *Netherlands Journal of Zoology*, **34**(1), 21-34.

Huijng, P.A. (1985) Architecture of the human gastrocnemius muscle and some functional consequences. *Acta Anatomica*, **123**, 101-107.

Levine, W.S., Zajac, F.E., Belzer, M.R., & Zomlefer, M.R. (1983). Ankle controls that produce a maximal vertical jump when other joints are locked. *IEEE Transactions on Autonomic Control*, **28**, 1008-1016.

Murray, W.M., Wyles, D.L., Buchanan, T.S., & Delp, S.L. (1996). Elbow muscle architecture and moment arms in differently sized specimens. In P. Crago & J.M. Winters (Eds.), *Biomechanics and neural control of movement* (pp. 61-62). New York: Engineering Foundation Conferences.

Nelder, J.A., & Mead, R. (1964). A simplex method for function optimization. *Computer Journal*, **7**, 308-313.

Otten, E. (1985). Some numerical reflections upon the simple planimetric muscle model of Huijing & Woittiez. *Netherlands Journal of Zoology*, **35**(3), 517-520.

Otten, E. (1988). Concepts and models of functional architecture in skeletal muscle. *Exercise and Sport Sciences Reviews*, **16**, 89-137.

Out, L., Vrijkotte, T.G.M., Soest, A.J. van, & Bobbert, M.F. (1996). Influence of structural properties of the human triceps surae muscle on the torque-angle relationship: A model study. *Journal of Biomechanical Engineering*, **118**, 17-25.

Pandy, M.G., Zajac, F.E., Sim, E., & Levine, W.S. (1990). An optimal control model for maximum height human jumping. *Journal of Biomechanics*, **24**, 1-10.

Pierrynowski, M.R., & Morrisson, J.B. (1985). A physiological model for the evaluation of muscular forces in human locomotion: Theoretical aspects. *Math Biosciences*, **75**, 69-101.

Pronk, G.M., & Helm, F.C.T. van der (1991). The palpator: An instrument for measuring the position of bones in three dimensions. *Journal of Medical Engineering and Technology*, **15**, 15-20.

Soest, A.J. van, Schwab, A.L., Bobbert, M.F., & Ingen Schenau, G.J. van (1993). The influence of the bi-articularity of the gastrocnemius muscle on vertical jumping achievement. *Journal of Biomechanics*, **26**, 1-8.

Spoor, C.W., Leeuwen, J.L. van, Meulen, W.J.T.M. van der, & Huson, A. (1991). Active force-length relationship of human lower-leg muscles estimated from morphological data: A comparison of geometric muscle models. *European Journal of Morphology*, **29**(3), 137-160.

Tredinnick, T.J., & Duncan, P.W. (1988). Reliability of measurements of concentric and eccentric isokinetic loading. *Physical Therapy*, **68**, 656-659.

Visser, J.J., Hoogkamer, J.E., Bobbert, M.F., & Huijing, P.A. (1990). Length and moment arm of human leg muscles as a function of knee and hip joint angles. *European Journal of Applied Physiology*, **61**, 453-460.

Walker, S.M., & Schrodt, G.R. (1974). I segment length and thin filament periods in skeletal muscle fibers of the rhesus monkey and the human. *Anatomical Records*, **178**, 63-82.

Wickiewicz, T.M.D., Roy, R.R., Powell, P.L., & Edgerton, V.R. (1983). Muscle architecture of the human lower limb. *Clinical Orthopedics and Related Research*, **179**, 275-283.

Willems, M.E.T., & Huijing, P.A. (1993). *Individual differences in length range of active force exertion by rat SMI are explained by variation in distribution of mean sarcomere lengths of its fibers*. From abstract book of the XIVth Congress of the International Society of Biomechanics (pp. 1464-1465), Lancaster, UK, April 5-10.

Yamaguchi, G.T., Sawa, A.G.U., Moran, D.W., Fessler, M.J., & Winters, J.M. (1990). A survey of human musculotendon actuator parameters. In J.M. Winters & S.L.Y. Woo (Eds.), *Multiple muscle systems* (pp. 717-773) New York: Springer Verlag.

Zuurbier, C.J., & Huijing, P.A. (1992). Influence of muscle geometry on shortening speed of fibre, aponeuroses and muscle. *Journal of Biomechanics*, **25**, 1017-1026.

Acknowledgments

We would like to thank G.C. Baan for his assistance in determining parameters, Ir. J. Harlaar for his introduction to the Kin-Com measurements, and Dr. H. Schutte for his support in the dissection room.